Article Type:	Invited Methods Collection - JoVE Produced Video
Manuscript Number:	JoVE61584R2
Full Title:	Dual-raster-scanning photoacoustic small-animal imager for vascular visualization
Keywords:	Photoacoustic imager; Small animal; Vascular visualization; Dual scanning; Wide-field imaging; Real-time imaging
Corresponding Author:	Fei Yang South China Normal University Guangzhou, Guangdong CHINA
Corresponding Author's Institution:	South China Normal University
Corresponding Author E-Mail:	yangfeidoudou@163.com
Order of Authors:	Fei Yang
	Zhiyang Wang
	Sihua Yang
Additional Information:	
Question	**Response**
Please indicate whether this article will be Standard Access or Open Access.	Standard Access (US$2,400)
Please indicate the **city, state/province, and country** where this article will be **filmed**. Please do not use abbreviations.	Guangzhou, Guangdong, China

1 **TITLE:**
2 **Dual Raster-Scanning Photoacoustic Small-Animal Imager for Vascular Visualization**
3

4 **AUTHORS AND AFFILIATIONS:**
5 Fei Yang[1,2], Zhiyang Wang[1,2], Sihua Yang[1,2]
6

7 [1]MOE Key Laboratory of Laser Life Science & Institute of Laser Life Science, College of
8 Biophotonics, South China Normal University, Guangzhou, China.
9 [2]Guangzhou Provincial Key Laboratory of Laser Life Science, College of Biophotonics, South China
10 Normal University, Guangzhou, China.
11

12 **Corresponding author:**
13 Sihua Yang   (yangsh@scnu.edu.cn)
14

15 **Email addresses of authors:**
16 Fei Yang   (yangfeidoudou@163.com)
17 Zhiyang Wang (wzy_0617@163.com)
18

19 **KEYWORDS:**
20 Photoacoustic imager, small animal, vascular visualization, dual scanning, wide-field imaging,
21 real-time imaging
22

23 **SUMMARY:**
24 A dual raster-scanning photoacoustic imager was designed, which integrated wide-field imaging
25 and real-time imaging.
26

27 **ABSTRACT:**
28 Imaging of vascular networks on small animals has played an important role in basic biomedical
29 research. Photoacoustic imaging technology has great potential for application in the imageology
30 of small animals. The wide-field photoacoustic imaging of small animals can provide images with
31 high spatiotemporal resolution, deep penetration, and multiple contrasts. Also, the real-time
32 photoacoustic imaging system is desirable to observe the hemodynamic activities of small-animal
33 vasculature, which can be used to research the dynamic monitoring of small-animal physiological
34 features. Here, a dual-raster-scanning photoacoustic imager is presented, featuring a switchable
35 double-mode imaging function. The wide-field imaging is driven by a two-dimensional motorized
36 translation stage, while the real-time imaging is realized with galvanometers. By setting different
37 parameters and imaging modes, in vivo visualization of small-animal vascular network can be
38 performed. The real-time imaging can be used to observe pulse change and blood flow change
39 of drug-induced, etc. The wide-field imaging can be used to track the growth change of tumor
40 vasculature. These are easy to be adopted in various areas of basic biomedicine research.
41

42 **INTRODUCTION:**
43 In the basic biomedical field, small animals can simulate human physiological function. Therefore,
44 small-animal imaging plays an important role in guiding the research of human homologous

45 diseases and seeking effective treatment[1]. Photoacoustic imaging (PAI) is a non-invasive imaging
46 technique combining the advantages of optical imaging and ultrasound imaging[2]. Photoacoustic
47 microscopy (PAM) is a valuable imaging method for basic research of small animal[3]. PAM can
48 easily obtain high-resolution, deep-penetration, high-specificity and high-contrast images based
49 on optical excitation and ultrasound detection[4].
50
51 A pulse laser with a specific wavelength is absorbed by endogenous chromophores of tissues.
52 Subsequently, the temperature of the tissue rises, which results in the production of photo-
53 induced ultrasonic waves. The ultrasonic waves can be detected by an ultrasonic transducer.
54 After signal acquisition and image reconstruction, the spatial distribution of the absorber can be
55 obtained[5]. On the one hand, the visualization of whole-organ vascular network requires a wide
56 field of view. The process of wide-field scanning usually takes a long time to ensure high-
57 resolution[6-8]. On the other hand, observing the hemodynamic activities of small animals requires
58 fast real-time imaging. The real-time imaging is beneficial to study the vital signs of small animals
59 in real time[9-11]. The field of view of real-time imaging is usually sufficiently small to ensure a high
60 update rate. Thus, there is often a tradeoff between achieving a wide field of view and real-time
61 imaging. Previously, two different systems were used for wide-field imaging or real-time imaging,
62 separately.
63
64 This work reports a dual raster-scanning photoacoustic imager (DRS-PAI), which integrated wide-
65 field imaging based on a two-dimensional motorized translation stage and real-time imaging
66 based on a two-axis galvanometer scanner. The wide-field imaging mode (WIM) is performed to
67 show vascular morphology. For the real-time imaging mode (RIM), there are currently two
68 functions. First, RIM can provide real-time B-scan images. By measuring the displacement of
69 vasculature along the depth direction, the characteristics of respiration or pulse can be revealed.
70 Second, the RIM can quantitatively measure the specific area in the WIM image. By providing
71 comparable images of local WIM regions, the details of the local change can be accurately
72 revealed. The system designs a flexible transition between wide-field imaging of vascular
73 visualization and real-time imaging of the local dynamic. The system is desirable in basic
74 biomedical research where there is a need for small-animal imaging.
75
76 **PROTOCOL:**
77 All animal experiments were performed in compliance with guidelines provided by the
78 institutional animal care and use committee of South China Normal University, Guangzhou,
79 China.
80
81 **1. System Setup**
82
83 1.1. Optical path (**Figure 1**)
84
85 1.1.1. Use a 532 nm pulse laser as the system laser source. Set the repetition rate of the laser to
86 10 kHz, the output energy to 100% and the trigger setting to external trigger using a user-defined
87 program.
88

89 1.1.2. Couple the laser beam to single-mode fiber (SMF) via an optical fiber coupler (FC1).
90 Collimate the laser beam using an optical fiber collimator (FC2) on a two-dimensional motorized
91 stage (Motor, maximum speed: 20 mm/s).
92
93 1.1.3. Deflect the laser beam using a two-axis galvanometer scanner (Galva). Use a moveable
94 mirror (M1) to reflect the beam. Focus the beam through a 4× objective lens (OL, Numerical
95 aperture: 0.1).
96
97 1.1.4. Use an XY translator mount (TM) to fix the self-made hollow ultrasonic transducer (UT,
98 Central frequency: 25 MHz; Bandwidth: more than 90%; Center hole: 3 mm) on the bottom of
99 the OL[12]. Pass the focused beam through the center hole of the ultrasonic transducer.
100
101 1.2. Scanning path
102
103 1.2.1. Lock the Galva using Field Programmable Gate Array (FPGA 2) during WIM. Set the
104 appropriate scanning range and scanning speed by a user-defined program.
105
106 1.2.2. Lock the Motor using a field-programmable gate array (FPGA 1) during RIM. Set the
107 scanning frequency and number of scanning points using FPGA 2. Use a user-defined program to
108 control the start and stop scanning.
109
110 1.3. Data acquisition
111
112 1.3.1. Use a 50-dB amplifier (AMP) to amplify the PA signal. Digitize the signal by the data
113 acquisition card (DAQ). Obtain the trigger signal through FPGA 1 or FPGA 2.
114
115 1.3.2. Use a graphics processing unit (GPU) to process data and display images in parallel[13].
116
117 1.4. CCD imaging system
118
119 1.4.1. Use a ring-shaped white LED (Color temperature: 6500 K; Illuminance: 40000 lux; Diameter:
120 7.5 cm) as a lighting source. Remove M1, use a fixed mirror (M2) to reflect the light.
121
122 1.4.2. Record the images using a CCD camera (6.3 million pixels) on the PA imaging system.
123 Display the images with a display software.
124
125 **2. System alignment**
126
127 2.1. Select a water tank (10 cm × 10 cm × 4.4 cm; bottom window: 3 cm × 3 cm). Cover the entire
128 water tank using a polyethylene membrane (membrane thick: 10 µm). Add sufficient ultrapure
129 water.
130
131 2.2. Place the water tank on the working stage.
132

2.3. Turn on the laser switch. Select the laser control program. Preheat for 5 min. Press the "ON" button on the pumping switch. Set the laser parameters as per step 1.1.1. Open the baffle of the laser.

2.4. Select the A-line collected program. Press the "Start" button to capture the single point signal and display amplitude and spectrum of the current A-line signal.

2.5. Place a blade at the bottom of the water tank. Immerse the bottom part of UT in the water tank for acoustic coupling. Avoid bubbles in the bottom part of UT.

2.6. Adjust the position of Galva, adjust XY translator between UT and OL to avoid oscillation signal, and make sure this is confocal.

2.7. Adjust the height of the working stage to maximize the amplitude of the signal, and determine the focus position.

3. Animal experiment

3.1. Use a 5–6 weeks old BALB/c mouse with a bodyweight of 20–30 g.

3.2. Anesthetize the animal using urethane (1 g/kg) injected intraperitoneally before the experiment.

3.3. Conduct transition between WIM and RIM.

3.3.1. Use a planar ultrasonic transducer. Shave the fur on the back of the mouse using a trimmer and depilatory cream. Place the mouse on the holder (8 cm × 2.8 cm × 2 cm) in prone position.

3.3.2. Allow the imaging region to be in contact with the polyethylene membrane using ultrasound gel. Avoid bubbles in the contact part.

3.3.3. Place the holder on the working stage for acoustic coupling. Follow steps 2.3–2.4 to start the laser and collect A-line signal. Follow steps 2.6–2.7 to align. Press "Stop" to end the collection after alignment.

3.3.4. Select the WIM program. Name the newly created folder. Set the scanning parameter at to 20 mm/s in the "Scanning Speed" tab, "20 mm*20 mm" in the "Scanning Area" tab, and "20" in the "Step" tab. Click the **Collect** button to start scanning.

3.3.5. Click the **Stop** button to end scanning after acquisition. Click **Return to Zero** to bring the Motor to zero. Close the laser baffle. Set the trigger setting to internal trigger. Press the **OFF** button for pumping switch.

176 3.3.6. Replace WIM trigger as RIM trigger and connect it to the external laser trigger. Press the
177 **ON** button for pumping switch. Set the trigger setting to the external trigger. Click the **Exit** button
178 to exit the WIM program.

180 3.3.7. Use step 2.4 to collect the A-line signal. Open the laser baffle. Follow steps 2.6–2.7 to align.
181 Press **Stop** to end collection after alignment.

183 3.3.8. Select the RIM program. Name the newly created folder. Click the **Collect** button to start
184 scanning.

186 3.3.9. Click the **Stop** button to end scanning after completing acquisition. Click the **Exit** button to
187 exit the RIM program.

189 3.4. Conduct WIM of vascular visualization.

191 3.4.1. Use a focused ultrasonic transducer (Central frequency: 25 MHz; Bandwidth: more than
192 90%; Focal length: 8 mm). Remove the hair of mice ear or scalp.

194 3.4.1.1. Use a scalpel to make a small incision on the lateral side of the cranial temporal top of
195 the mouse (depth to the skull). Use ophthalmic scissors to start from this incision. Cut the scalp
196 around the outer side of the skull. Compress the bleeding point to stop bleeding. Wash the
197 wound with normal saline. Place the mouse on the holder.

199 3.4.2. Allow the imaging region to be in contact with the polyethylene membrane using
200 ultrasound gel. Avoid bubbles in the contact region (**Supplementary Figure 1**).

202 3.4.3. Place the holder on the work stage for acoustic coupling. Use steps 2.3–2.4 to open laser
203 and collect A-line signal. Use step 2.6–2.7 to align. Press **Stop** to end collection after alignment.

205 3.4.4. Select WIM program. Name the newly created folder. Set the scanning parameter to "10
206 mm/s" in the "Scanning Speed" tab, "10 mm*10 mm" under the "Scanning Area" tab, and "10"
207 in the "Step" tab. Click the **Collect** button to start scanning.

209 3.4.5. Click the **Stop** button to end scanning after completing acquisition. Click the **Return to Zero**
210 to make the Motor return to zero. Click the **Exit** button to exit the WIM program.

212 3.5. Conduct RIM for dynamic monitoring of small animals.

214 3.5.1. Shave the hair of the mouse abdomen. Place the mouse on the holder in supine position.

216 3.5.2. Allow the imaging region to be in contact with the polyethylene membrane using
217 ultrasound gel. Avoid bubbles in the contact region.
218

3.5.3. Place the holder on the work stage for acoustic coupling. Perform steps 2.3–2.4 to start the
220 laser and collect A-line signal. Perform step 2.6–2.7 to align. Press **Stop** to end collection after
221 alignment.
222
223 3.5.4. Select the RIM program. Name the newly created folder. Click the **Collect** button to start
224 scanning.
225
226 3.5.5. Click the **Stop** button to end scanning after completing acquisition. Click the **Exit** button to
227 exit the RIM program.
228
229 3.6. Use the RIM data for reconstruction of the maximum amplitude projection (MAP) along the
230 depth direction by user-defined program. Observe the dynamic changes in the animal.
231
232 **REPRESENTATIVE RESULTS:**
233 The schematic of the DRS-PAI is shown in **Figure 1**. The system allows flexible and repeatable
234 switching between WIM with RIM. The acquired PA signal is processed quickly to generate PA B-
235 Scan and MAP images. The CCD camera can provide photographs of samples.
236
237 All components of the DRS-PAI are integrated and assembled in an imager setup (**Figure 2**),
238 making it easy to assemble and operate. In the WIM, continuous raster scanning of a two-
239 dimensional motorized stage is used. The signal of the running stage is recorded. The data
240 acquisition proceeded during uniform translation of the stage. In the RIM, a two-axis
241 galvanometer scanner was used. The data were collected synchronously with the Galva scanning
242 (**Figure 3**).
243
244 Here, the vascular images of samples with each imaging mode were collected. **Figure 4A** shows
245 the MAP image of the mouse back in WIM. The imaging time was about 33 min. **Figure 4B** shows
246 B-scan images of mouse back during RIM. The whole process of RIM is shown in **Video 1**. Then, a
247 focused ultrasonic transducer was used. The vascular networks of the mouse ear and brain are
248 shown in **Figure 5**. The imaging time was about 16 min. This demonstrates the ability of DRS-PAI
249 to image wide-field vasculature. In addition, **Figure 6A** shows that the imaging range contains a
250 vessel. The imaging range of RIM is about 100 μm due to the use of the focused ultrasonic
251 transducer. The displacement image along the depth direction of the mouse abdomen versus
252 time is shown in **Figure 6B**. **Video 2** shows the process of vascular displacement and obtaining
253 the current pulse or respiration curve.
254
255 **FIGURE AND TABLE LEGENDS:**
256
257 **Figure 1: The schematic of DRS-PAI system.**
258
259 **Figure 2: The design of DRS-PAI system**. (**A**) The photograph of DRS-PAI system. (**B**) The panel
260 shows a photograph of the setup for laser path assembly. (**C**) The panel shows the 3D model for
261 laser path assembly. (**D**) The panel shows the two-axis fast galvanometer scanner assembly. (**E**)
262 The panel shows the probe assembly. (**F**) The panel shows the CCD optical path assembly.

Figure 3: The setup of scan for different imaging modes. (**A**) The scan path of WIM. (**B**) The scan path of RIM. (**C**) The trigger setup of two imaging modes.

Figure 4: The photoacoustic WIM and RIM of the mouse back. (**A**) The MAP image of mouse back in WIM. (**B**) The B-Scan images of mouse back in RIM.

Figure 5: The photoacoustic WIM of a mouse. (**A**) The MAP image of the mouse ear in WIM. (**B**) The MAP image of the mouse brain in WIM.

Figure 6: The photoacoustic RIM of the mouse abdomen. (**A**) The B-scan images of the mouse abdomen in RIM. (**B**) The MAP image along the depth direction of the mouse abdomen versus time in RIM.

Video 1: The process of RIM of the mouse back.

Video 2: The process of MAP image along the depth direction of the mouse abdomen versus time.

Supplementary Figure 1: The part of the imaging region in contact with the polyethylene membrane.

DISCUSSION:

Here we presented a dual raster-scanning photoacoustic small-animal imager for noninvasive vascular visualization which was designed and developed to capture the structure of the vasculature and the related dynamic change of blood. The advantage of DRS-PAI is that it integrates the WIM and the RIM into one system, which makes it easier to study vascular dynamic and vascular network structure of small animals. The system can provide high-resolution wide-field vascular visualization and real-time blood dynamics.

In the current system, the optical excitation was implemented with a single-wavelength light source. A future multi-wavelength system would provide other parameters such as blood oxygen saturation. Further, a special image processing algorithm can be developed for quantitative analysis, including estimating vascular diameter, vascular density, vascular tortuosity, etc. The quantitative analysis can provide valuable information for early diagnosis and treatment of diseases.

In summary, the system enables researchers to obtain high-dimensional physiological and pathological insights into small-animal research with biomedical relevance. The system can be adapted to most small-animal research settings, include but not limited to, imaging of angiogenesis, tumor microenvironments, hemodynamic, functional connections in the brain, microcirculation, drug responses, and therapy responses. Critical steps within the protocol include the design of the dual scanning structure, the confocal adjustment of the optical and acoustic focus in the WIM, and center point adjustment of the sound field in the RIM.
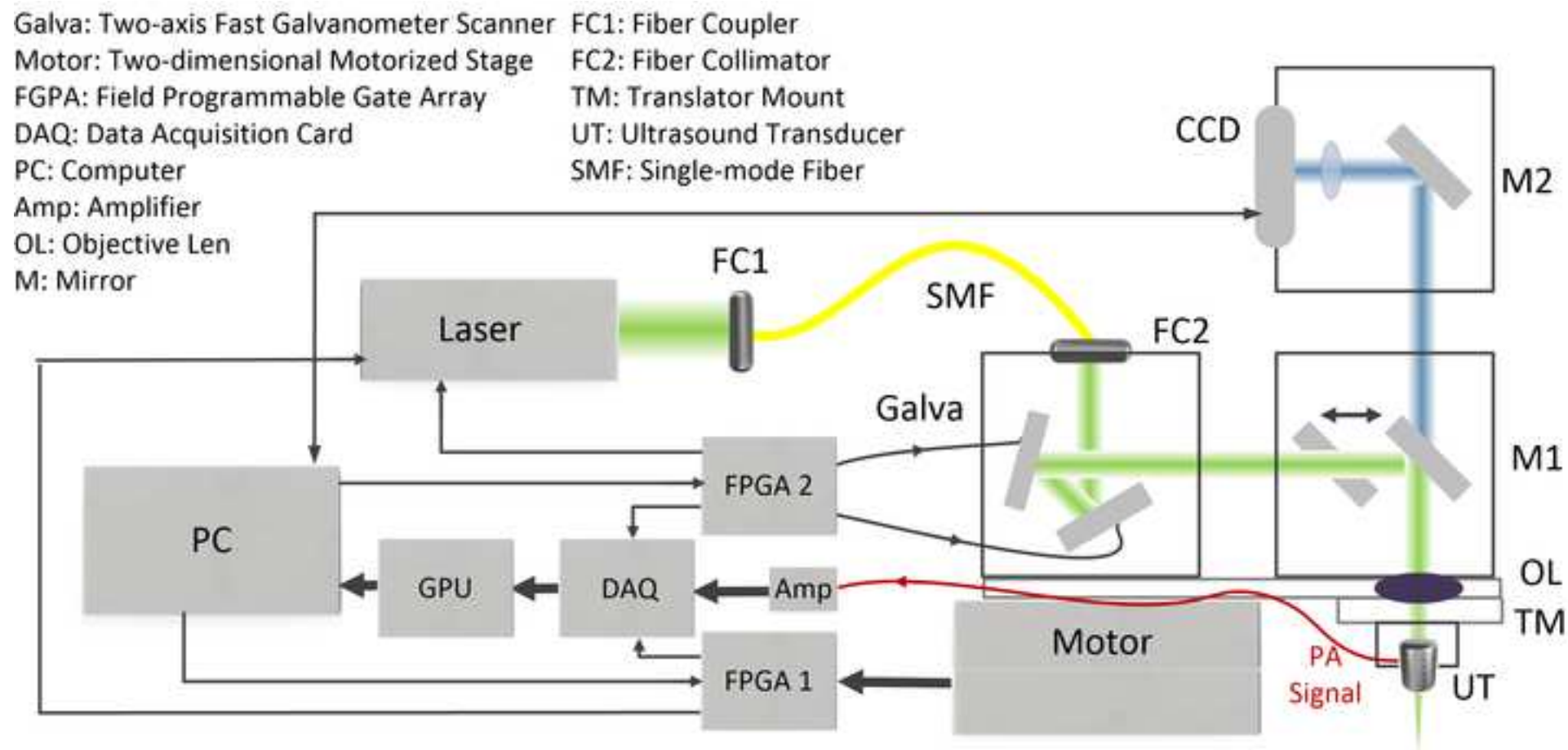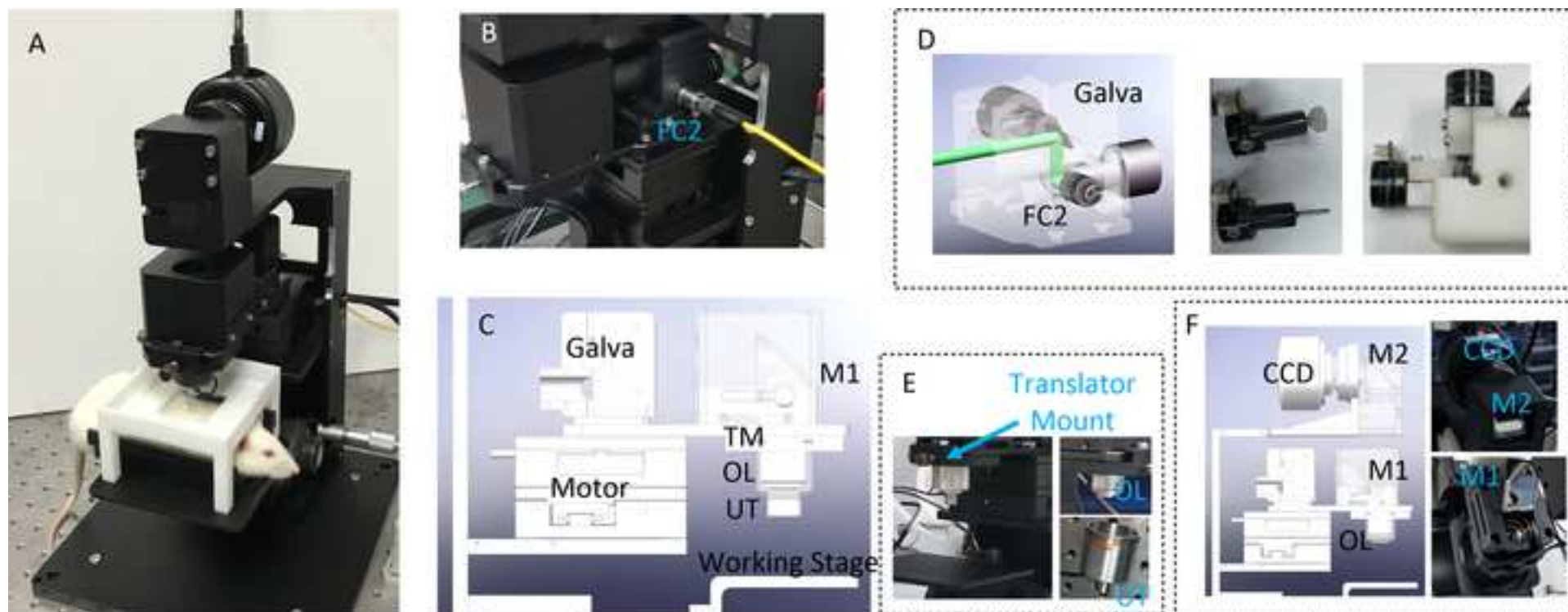
307

DISCLOSURES:

All animal experiments were performed according to the approved guidelines and regulations of the Institutional Animal Care and Use Committee. The authors have no relevant financial interests in the manuscript and no other potential conflicts of interest to disclose.
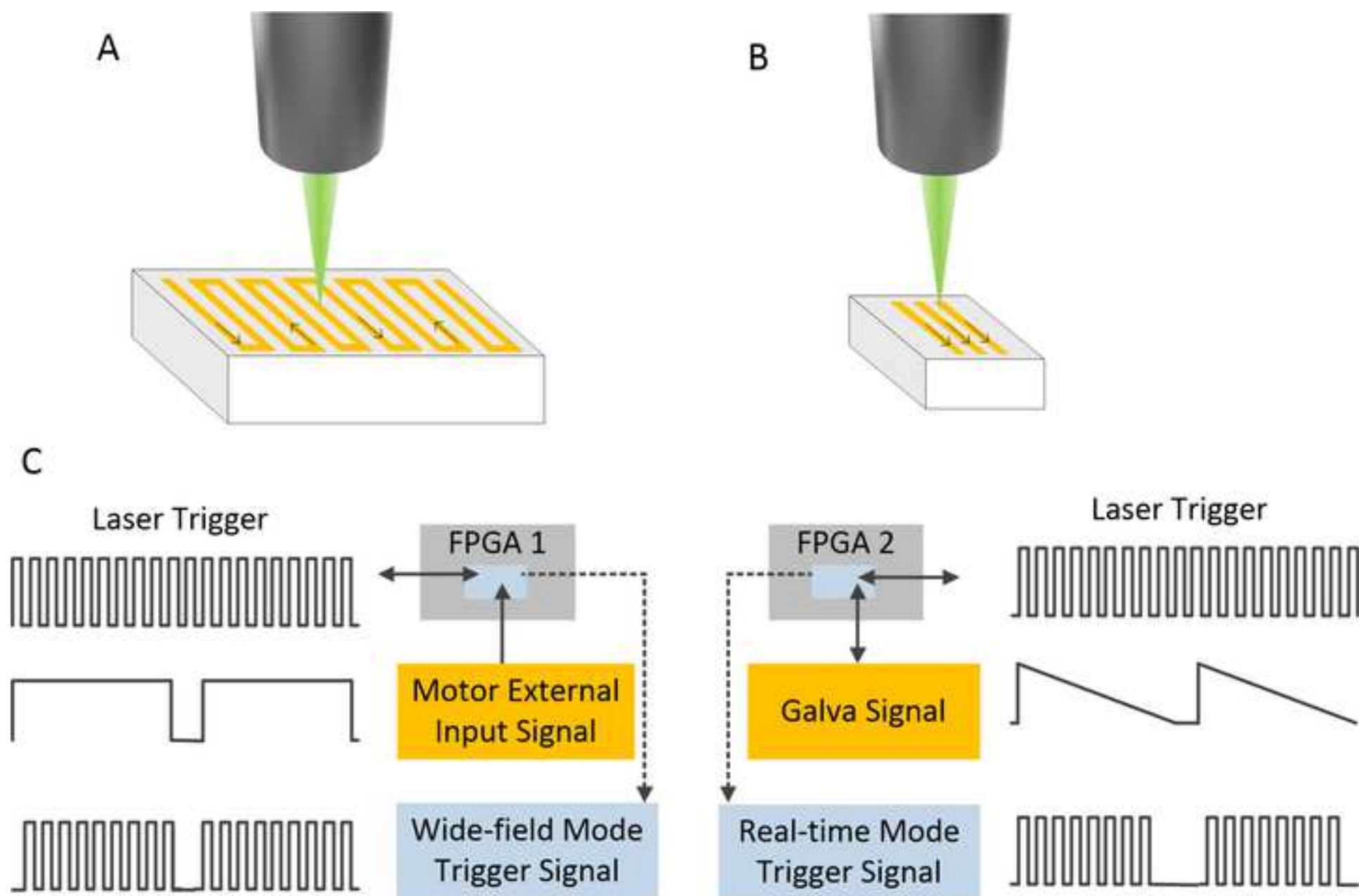
REFERENCES:

1. Li, L., et al. Single-impulse panoramic photoacoustic computed tomography of small-animal whole-body dynamics at high spatiotemporal resolution. *Nature Biomedical Engineering*. **1**(5), 0071 (2017).

2. Jeon, S., Kim, J., Lee, D., Baik, J. W., Kim, C. Review on practical photoacoustic microscopy. *Photoacoustics.* **15**, 100141 (2019).

3. Baik, J. W., et al. Super wide-field photoacoustic microscopy of animal and humans *in vivo*. *IEEE Transactions on Medical Imaging.* **39** (4), 975-984 (2019).

4. Omar, M., Aguirre, J., Ntziachristos, V. Optoacoustic mesoscopy for biomedicine. *Nature Biomedical Engineering*. **3** (5), 354-370 (2019).

5. Lin, L., et al. Single-breath-hold photoacoustic computed tomography of the breast. *Nature Communications*. **9** (1), 2352 (2018).

6. Yang, F., et al. Wide-field monitoring and real-time local recoding microvascular networks on small animals with a dual-raster-scanned photoacoustic microscope. *Journal of Biophotonics*. **13** (6), e202000022 (2020).

7. Sun, J., Zhou, Q., Yang, S. Label-free photoacoustic imaging guided sclerotherapy for vascular malformations: a feasibility study. *Optics Express*. **26** (4), 4967-4978 (2018).

8. Xu, D., Yang, S., Wang, Y., Gu, Y., Xing, D. Noninvasive and high-resolving photoacoustic dermoscopy of human skin. *Biomedical Optics Express*. **7** (6), 2095-2102 (2016).

9. Zhang, W., et al. Miniaturized photoacoustic probe for *in vivo* imaging of subcutaneous microvessels within human skin. *Quantitative Imaging in Medicine and Surgery.* **9** (5), 807-814 (2019).

10. Chen, Q., et al. Ultracompact high-resolution photoacoustic microscopy. *Optics Letters*. **43** (7), 1615-1618 (2018).

11. Lan, B., et al. High-speed widefield photoacoustic microscopy of small-animal hemodynamics. *Biomedical Optics Express*. **9**, 4689-4700 (2018).

12. Ma, H., Yang, S., Cheng, Z., Xing, D. Photoacoustic confocal dermoscope with a waterless coupling and impedance matching opto-sono probe. *Optics Letters*. **42** (12), 2342-2345 (2017).

13. Kang, H., Lee, S. W., Lee, E. S., Kim, S. H., Lee. T. G. Real-time GPU-accelerated processing and volumetric display for wide-field laser-scanning optical-resolution photoacoustic microscopy. *Biomedical Optics Express*. **6** (12), 4650-4660 (2015).
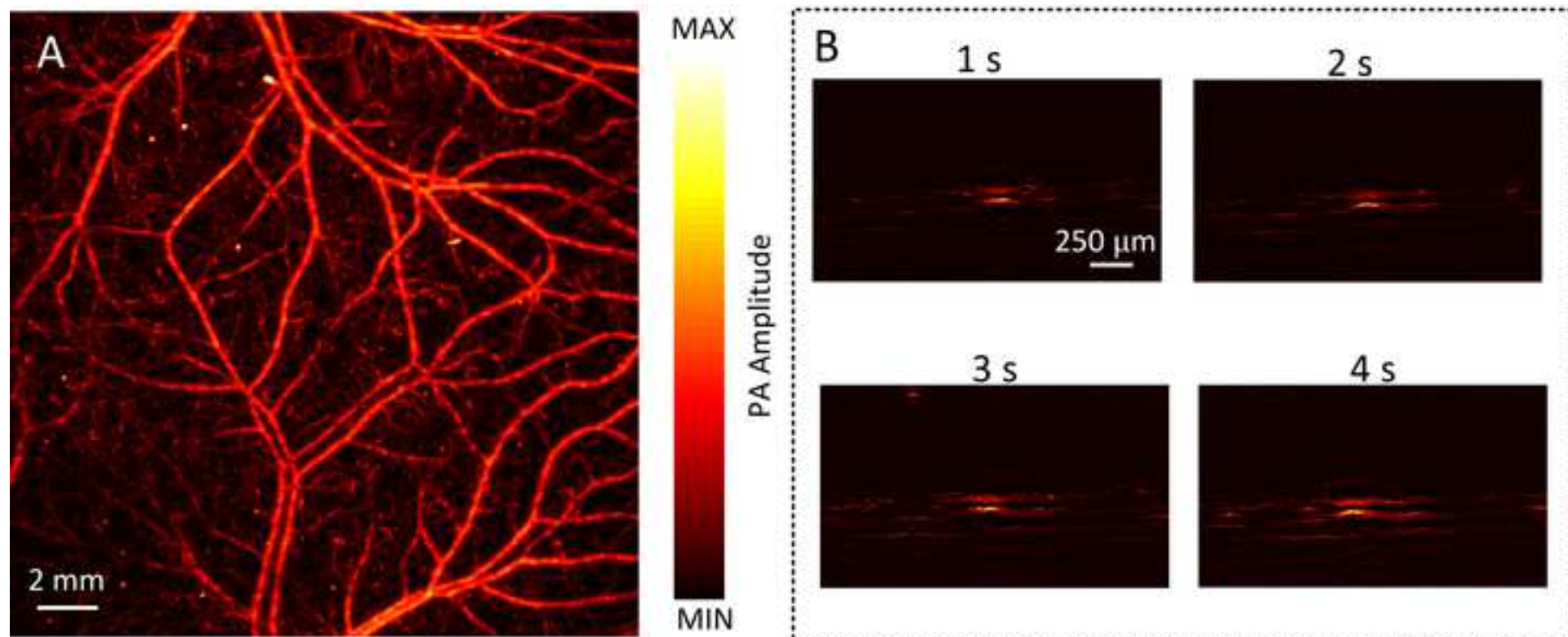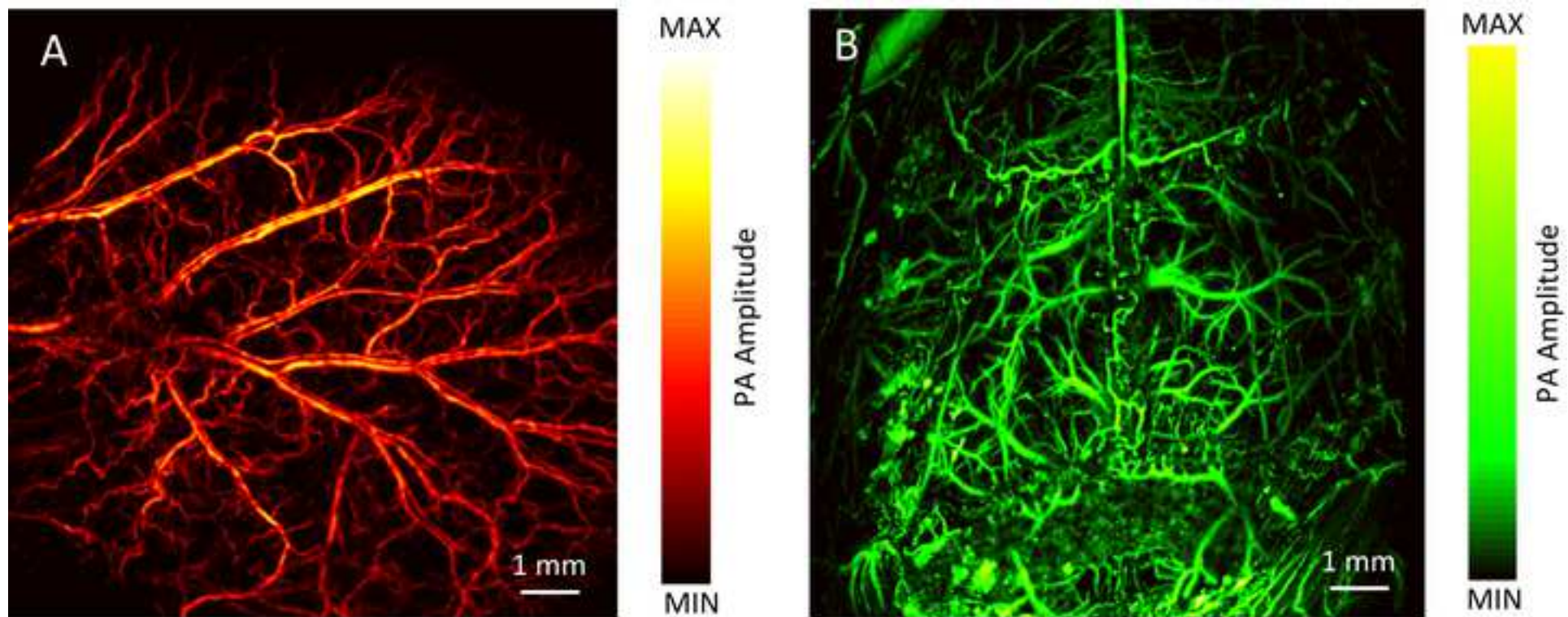
Figure 1   Click here to access/download;Figure;Figure1.psd ⬇

Galva: Two-axis Fast Galvanometer Scanner FC1: Fiber Coupler
Motor: Two-dimensional Motorized Stage FC2: Fiber Collimator
FGPA: Field Programmable Gate Array TM: Translator Mount
DAQ: Data Acquisition Card UT: Ultrasound Transducer
PC: Computer SMF: Single-mode Fiber
Amp: Amplifier
OL: Objective Len
M: Mirror

Figure 2

A

B   FC2

C   Galva   M1
     TM
     OL
Motor   UT
     Working Stage

D   Galva   FC2

E   Translator   Mount   OL

F   CCD   M2   CCD   M2   M1   M1   OL

Figure 3 Click here to access/download;Figure;Figure3.psd ⬇

A

B

C

Laser Trigger

FPGA 1

Motor External
Input Signal

Wide-field Mode
Trigger Signal

FPGA 2

Galva Signal

Real-time Mode
Trigger Signal

Laser Trigger

Figure 4

Figure 5

Figure 6

A

250 µm

MAX

PA Amplitude

B

MIN

0 s (The first B-Scan image)
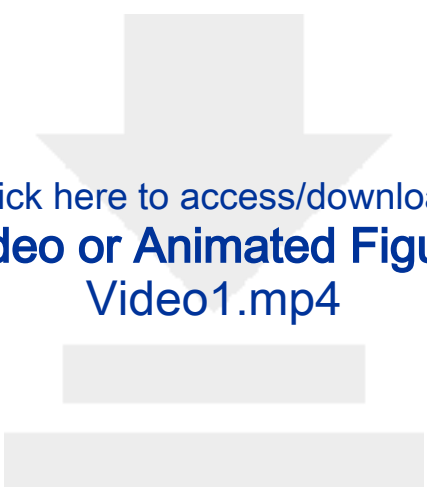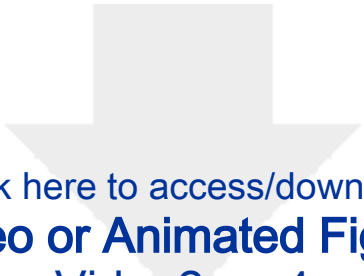
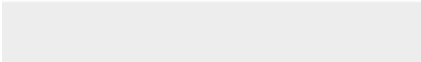6 s (The 240th B-Scan image)

Time (s)

Video 1

Click here to access/download

Video or Animated Figure
Video1.mp4

Click here to access/download
Video or Animated Figure
Video2.mp4

Name of Material/ Equipment	Company
12 bit multi-purpose digitizer	Spectrum
A-line collected program	National Instrument
Amplifier	RF Bay
Depilatory Cream	Veet
Fiberport Coupler	Thorlab
Field Programmable Gate Array	Altera
Fixed Focus Collomation Packages	Thorlabs
Foused ultrasonic transducer	Self-made
Graphics Processing Unit	NVIDIA
Holder	Self-made
Laser control program	National Instrument
Mice	Guangdong Medical Laboratory Animal Center
Microscope camera	Mshot
Microscope Objective	Daheng Optics
Mirror	Daheng Optics
Moving Magnet Capacitive Detector Galvanometer Scanner	Century Sunny
Mshot image analysis system	Mshot
Normal Saline	CR DOUBLE-CRANE
Ophthalmic Scissors	SUJIE
Planar ultrasonic transducer	Self-made
Plastic Wrap	HJSJLSL
Program Control Software	National Instrument
Pulsed Q-swithched Laser	Laser-export
Real-time imaging program	National Instrument
Ring-shaped white LED	Self-made
Shaver	Codos
Single-Mode Fibers	Nufern
Surgical Blade	SUJIE
Surgical Scalpel	SUJIE
Translation Stage	Jiancheng Optics
Ultrasonic Transducer	Self-made
Ultrasound gel	GUANGGONG PAI

Urethane	Tokyo Chemical Industry
Water tank	Self-made
Wide-field imaging program	National Instrument
XY Translator Mount	Self-made

Catalog Number	Comments/Description
M3i.3221	Data acquisition card
LabVIEW	User-defined program
LNA-650	Amplifier
33-II	Animal depilatory
PAF-X-7-A	Fiber Coupler
Cyclone IV	Trigger Control
F240FC-532	Fiber Collimator
GeForce GTX 1060	Processing data
	Animal fixation
LabVIEW	User-defined program
BALB/c	Animal Model
MS60	CCD camera
GCO-2111	Objective Lens
GCC-1011	Moveable/Fixed Mirror
S8107	real-time scanner
	Display software
H34023609	Normal Saline
	Scalp Remove
	Polyethylene Membrane
LabVIEW	User-defined Program
DTL-314QT	532-nm pulse Laser
LabVIEW	User-defined program
CP-9200	Animal Shaver
460-HP	Single-mode fiber
11	Blade
7	Scalp Remove
LS2-25T	wide-field scanning stage
ZC4252418	Acoustic Coupling

C0028   Animal Anestheized

LabVIEW   User-defined program

Dear Editor,

We would like to express our great gratitude to you and reviewers for the insightful comments and constructive suggestions. Here, we submit a revised version of our manuscript with the title "Dual-raster-scanning photoacoustic small-animal imager for vascular visualization" (Manuscript ID JoVE61584), which has been modified according to the editor and reviewer's suggestions. We have made the best efforts to revise the manuscript, and hope that these changes can lead to the acceptance of the manuscript.

We state that all authors have read and agreed with the contents of the revised manuscript and there is no financial interest to report. The manuscript, containing the original research results, has not been and will not be submitted elsewhere for publication. A point-by-point response to the reviewer's comments is attached as follows.

Thanks very much for your attention to the work.

With best regards,
Yours sincerely,
Fei Yang, Zhiyang Wang, Sihua Yang
MOE Key Laboratory of Laser Life Science
& Institute of Laser Life Science
South China Normal University, Guangzhou 510631, CHINA
E-mail: yangfeidoudou@163.com

Point-by-point response to reviews' comments

NOTE: All authors have carefully studied the comments of Reviewers #1 and #2. The changes in the revised manuscript are listed below each the reviewers' comment.

Reviewer #1:

This manuscript "Dual-raster-scanning photoacoustic small-animal imager for vascular visualization" introduced a photoacoustic microscopy (PAM) system that integrates the wide-field mode and real-time mode. This manuscript well explained the system configuration and provided effective visual materials. However, this paper needs improvement, and some details remain with the reader's imagination. Thus, I recommend publishing this paper if the following comments could be addressed.

Response:

We appreciate you for the constructive comments and suggestions. The manuscript has been revised according to your suggestions. Point-by-point responses are attached as follows.

1. Comment

B-mode is already available in wide-field mode. Despite the fast speed, the real-time mode can provide quite small FOV (~100 μm). Please provide a more detailed benefit in the integration of the motor- and galvanometer-based scanning systems.

Response:

Thanks for your suggestion. The DRS-PAI provides a flexible transition from wide-field monitoring the vasculature to real-time imaging of local dynamic *in vivo*. In the wide-field mode, wide FOV images are presented to show vascular morphology. For the real-time mode, there are currently two applications. First, the real-time B-scan images can be provided. So, the displacement of vascular along the depth direction can

be measured to reveal the characteristics of respiration or pulse. Second, the specific area in wide-field image can be quantitatively measured. So, the comparable images of different regions at the same period can be provided to accurately reveal the details of local change. We have added relevant descriptions in the revised manuscript (**Introduction Section**).

Line 68-74: "Combining wide-field imaging and real-time imaging will benefit basic research. In the wide-field mode, wide field images are presented to show vascular morphology. For the real-time mode, there are currently two applications. First, the real-time B-scan images can be provided. The displacement of vascular along the depth direction can be measured to reveal the characteristic of respiration or pulse. Second, the specific area in wide-field image can be quantitatively measured. The comparable images of different regions at the same period can be provided to accurately reveal the details of local change."

2. Comment

In the introduction section, the authors mentioned the principal and advantages of photoacoustic imaging (PAI). Please consider citing the following paper:

A. Jeon, Seungwan, et al. "Review on practical photoacoustic microscopy." Photoacoustics (2019):100141.

Response:

Thanks for your comments. We have added relevant contents in the revised manuscript (**Introduction Section**).

Line 51: "Photoacoustic imaging (PAI), as a non-invasive imaging technique combining the advantages of optical imaging and ultrasound imaging[2]."

2. Jeon, S., Kim, J., Lee, D., Baik, J. W., Kim, C. Review on practical photoacoustic microscopy. *Photoacoustics.* 15, 100141 (2019).

3. Comment

Please provide the detailed model name of the motor stage, OL and CCD, etc. The author also need to provide the following specification of the components.

A. Objective lens: The numerical aperture

B. Ultrasound transducer: Center frequency, Bandwidth, Inner hole size, Focal Length

C. Motor stage: Maximum speed

Response:

Thanks for your helpful advice. The detailed model name of the motor stage, OL and CCD were described in the **Table of materials**. The numerical aperture of objective lens is 0.1. The self-made single-element ultrasonic transducer is employed for photoacoustic detection with central frequency of 25 MHz, the bandwidth of more than 90%, the diameter of the element is 10 mm which is with a 3 mm center hole for the exit of the laser beam. Two types of ultrasonic transducers were used in the paper, including a planar ultrasonic transducer and a focused ultrasonic transducer. Particularly, the focal length of focused ultrasonic transducer is 8 mm. The maximum speed of the motor stage is 20 mm/s.

We have added relevant description in the revised manuscript (**protocol section**).

A. Line 98: "1.1.3 Deflect the laser beam by two-axis fast galvanometer scanner (Galva). Use a moveable mirror (M1) to reflect the beam pass through a 4× objective lens (OL, Numerical aperture: 0.1) for focusing"

B. Line 102: "1.1.4 Fix the self-made hollow single-element ultrasonic transducer (UT, Central frequency: 25 MHz; Bandwidth: more than 90%; Center hole: 3 mm) at the bottom of objective using a XY translator mount (TM), to pass the focused beam by the center hole of the ultrasonic transducer."

Line 186: "3.4.1 Remove the hair of mice ear and scalp. Remove the scalp of one of the mice. Use a focused ultrasonic transducer (the focal length: 8 mm)."

C. Line 94: "1.1.2 Collimate the laser beam using an optical fiber collimator (FC2) at the above of two-dimensional motorized stage (Motor, Maximum speed: 20 mm/s)."

4. Comment

Please provide the imaging time to acquire figures 4 and

Response:

Thank you for reminding me of the point. The repetition frequency of laser is 10 kHz.

Figure 4A shows PA MAP image in wide-field imaging. Among them, the scanning range is 20 mm* 20 mm, the scanning speed is 20 mm/s, the step distance on y-axis is 10 μm. A total of 2000 B-Scan images were collected. Thus, the imaging time takes about 33 minutes. Figure 4B shows B-Scan images in real-time imaging. The update frequency is 24 Hz. Figure 5A and 5B shows that the scanning range is 10 mm* 10 mm, the scanning speed is 10 mm/s, and the step distance on y-axis is 10 μm. A total of 1000 B-Scan images were collected. Thus, the imaging time takes about 16 minutes. We have added relevant description in the revised manuscript (**Representative Results Section**). Line 246: "Figure 4A shows the PA MAP image of mouse back in the wide-field imaging mode. The imaging time takes about 33 minutes."

Line 250: "Figure 5 shows the vascular visualization of mouse ear and brain. The imaging time takes about 16 minutes, respectively."

Reviewer #2:

The authors present an integrated dual-raster-scanning photoacoustic imager with two in one set-up.

Major Concerns:

Nil

Minor Concerns:

Any quantitative analysis available?

Response:

Thanks for your comments. The article is mainly about the system operation and experiment process. For the quantitative analysis of resulting images, we developed specialized image processing algorithm, including vascular diameter, vascular density, and vascular tortuosity. Among them, the vascular diameter is the distance between the vertical line passing through the vascular skeleton and the two points where vascular boundary intersects. The vascular density is represented as the ratio of all vascular pixels to the overall pixels of region of interest by binarizing the image. The vascular tortuosity is assessed by measuring the ratio between the actual path length of a vascular

segment in each subdomain and the linear distance between the two ends of the vascular. Another article by the author has a detailed introduction and results of the processing analysis (Reference 6). We have added relevant description in the revised manuscript (**Discussion section**).

Line 295: "the special image processing algorithm can be developed for quantitative analysis. The quantitative analysis, including vascular diameter, vascular density, vascular tortuosity etc., can provide valuable information for early diagnosis and treatment of diseases."

6. Yang, F., et al. Wide-field monitoring and real-time local recoding microvascular networks on small animals with a dual-raster-scanned photoacoustic microscope. *Journal of Biophotonics*. (2020).